Inhibition of the Broad Spectrum Nonmetallocarbapenamase of Class A (NMC-A) -Lactamase from Enterobacter cloacae by Monocyclic -Lactams* S

Lionel Mourey, Lakshmi Kotra, John Bellettini , Alexey Bulychev, Michael O'brien , Marvin Miller , Shahriar Mobashery, Jean-Pierre Samama

THE JOURNAL OF BIOLOGICAL CHEMISTRY
Vol. 274, No. 36, Issue of September 3, pp. 25260–25265, 1999

Printed in U.S.A.

Inhibition of the Broad Spectrum Nonmetallocarbapenamase of Class A (NMC-A) β-Lactamase from *Enterobacter cloacae* by Monocyclic β-Lactams*[S]

(Received for publication, March 26, 1999)

Lionel Mourey‡§, Lakshmi P. Kotra§¶, John Bellettini‖, Alexey Bulychev¶, Michael O'Brien‖, Marvin J. Miller‖, Shahriar Mobashery¶, and Jean-Pierre Samama‡****

From the ‡Groupe de Cristallographie Biologique, Institut de Pharmacologie et de Biologie Structurale du CNRS, 205 Route de Narbonne, 31077 Toulouse Cedex, France, the ¶Department of Chemistry, Wayne State University, Detroit, Michigan 48202, and the ‖Department of Chemistry and Biochemistry, University of Notre Dame, Notre Dame, Indiana 46556

β-Lactamases hydrolyze β-lactam antibiotics, a reaction that destroys their antibacterial activity. These enzymes, of which four classes are known, are the primary cause of resistance to β-lactam antibiotics. The class A β-lactamases form the largest group. A novel class A β-lactamase, named the nonmetallocarbapenamase of class A (NMC-A) β-lactamase, has been discovered recently that has a broad substrate profile that included carbapenem antibiotics. This is a serious development, since carbapenems have been relatively immune to the action of these resistance enzymes. Inhibitors for this enzyme are sought. We describe herein that a type of monobactam molecule of our design inactivates the NMC-A β-lactamase rapidly, efficiently, and irreversibly. The mechanism of inactivation was investigated by solving the x-ray structure of the inhibited NMC-A enzyme to 1.95 Å resolution. The structure shed light on the nature of the fragmentation of the inhibitor on enzyme acylation and indicated that there are two acyl-enzyme species that account for enzyme inhibition. Each of these inhibited enzyme species is trapped in a distinct local energy minimum that does not predispose the inhibitor species for deacylation, accounting for the irreversible mode of enzyme inhibition. Molecular dynamics simulations provided evidence in favor of a dynamic motion for the acyl-enzyme species, which samples a considerable conformational space prior to the entrapment of the two stable acyl-enzyme species in the local energy minima. A discussion of the likelihood of such dynamic motion for turnover of substrates during the normal catalytic processes of the enzyme is presented.

β-Lactamases are the primary cause of resistance to β-lactam antibiotics (1). These enzymes hydrolyze the β-lactam moiety of β-lactam antibiotics, and by so-doing, render them inactive. There are four classes of these enzymes, of which the class A is the largest group (1). The active-site serine in the class A β-lactamases undergoes acylation by the substrate and the acyl-enzyme intermediate is subsequently hydrolyzed to give substrate turnover (1, 2). Class A enzymes perform this task with their preferred substrates, penicillins, at the diffusion limit (3). Many of the "parental" β-lactamases of class A, such as the TEM-1 β-lactamase, have undergone mutations that impart to them an increase in the breadth of their substrate profile (1), as well as the ability to avoid being inhibited by the known clinical inhibitors. This is currently a serious clinical challenge.

One new class A β-lactamase, designated NMC-A[1] (4), and the highly homologous Sme-1 (5) and IMI-1 (6) β-lactamases, enjoy an unusually broad substrate profile, which includes penicillins, cephalosporins, and carbapenems (4, 7). Currently, carbapenem antibiotics such as imipenem are considered antibiotics of last resort, and the advent of enzymes that turn them over efficiently bodes poorly for the prospects of continued clinical utility of these versatile antibacterials.

The x-ray structure of the NMC-A enzyme, and its comparison to that of the classical class A enzyme (8, 9), showed that the carbapenamase activity of the NMC-A β-lactamase could be attributed to the displacement of Asn-132. The subtle relocation of this residue in the active site by a mere 1 Å, enlarges the substrate-binding site to accommodate the 6α-hydroxyethyl substituent of carbapenems, allowing the turnover process to take place (9). These observations were the basis for the design of a novel inactivator for the NMC-A β-lactamase, namely 6α-hydroxypropylpenicillanate (9). The x-ray structure determination of the complex of the NMC-A β-lactamase and the inhibitor illustrated that inactivation of the enzyme arose from interactions between the protein and inhibitor that prevented the approach of the hydrolytic water to the ester of the acyl-enzyme intermediate (9).

We disclose herein inhibition of the NMC-A β-lactamase by a set of monobactam inhibitors. These are effective inactivators for this enzyme, and their mechanism of action is distinct compared with that of 6α-hydroxypropylpenicillanate, which was reported earlier (9). The mechanistic implications of interactions of the NMC-A β-lactamase and one of the inhibitors of our design are addressed by the determination of the crystal structure of the complex, as well as by computational molecular dynamics simulations.

* The work in France was supported in part by INSERM (CRE Contract 930612), the Region Midi-Pyrenees (Contract 9200843), and CNRS (to J. P. S.). The work in the United States was supported by the National Institutes of Health and National Science Foundation (to S. M.) and Eli Lilly and Co. (to M. J. M.). The costs of publication of this article were defrayed in part by the payment of page charges. This article must therefore be hereby marked "*advertisement*" in accordance with 18 U.S.C. Section 1734 solely to indicate this fact.

[S] The on-line version of this article (available at http://www.jbc.org) contains the details of the synthetic procedures and additional descriptions of kinetic experiments.

§ The first two authors made equal contributions to the manuscript.

** To whom correspondence should be addressed. Tel.: 313-577-3924; Fax: 313-577-8822; E-mail: som@mobashery.chem.wayne.edu (for S. M.) or Tel.: 33-561-175-444; Fax: 33-561-175-448; E-mail: samama@ipbs.fr (for J.-P. S.).

[1] The abbreviations used are: NMC-A, nonmetallocarbapenamase of class A; 4-morpholineethanesulfonate.

TABLE I
X-ray diffraction data processing statistics given for the entire resolution range and for the highest resolution shell

	36.5–1.95 Å	2.06–1.95 Å
Number of measurements	68,848	9216
Number of unique reflections	20,566	2898
Completeness (%)	99.6	98.5
R_{sym} (%)	6.3	11.4
$\langle I/\mathrm{sd}(I)\rangle$	8.1	6.2

EXPERIMENTAL PROCEDURES

The NMC-A β-lactamase was purified to homogeneity according to a literature procedure (8). Cephaloridine was purchased from Sigma. Syntheses of compounds **1** and **6** were reported previously (10), and those for the remainder of the inhibitors are given in the Supplementary Material available in the on-line version. Spectrophotometric studies were performed on a Hewlett-Packard 8453 diode array instrument. Calculations were performed by the MS Excel program.

Kinetic Experiments—A 1.0-ml assay mixture typically consisted of 0.5 mM cephaloridine in 100 mM sodium phosphate, pH 7.0. Hydrolysis of the β-lactam ring of cephaloridine was monitored at 290 nm ($\Delta\epsilon_{290}$ = 2070 M^{-1} cm^{-1}) upon addition of the enzyme (final concentration was typically 5 nM).

Inactivation experiments were performed as follows. An aliquot of the stock solution of the inactivator (100 μM in *p*-dioxane) was added to the NMC-A β-lactamase (0.4 μM final concentration) in 100 mM sodium phosphate, pH 7.0, at 4 °C (10% *p*-dioxane final). Portions (10 μl) were removed from the mixture at time intervals and were diluted 100-fold into the assay mixture containing 0.5 mM cephaloridine. The enzyme activity was monitored until cephaloridine was entirely consumed. The remaining enzyme activity was calculated from the initial linear portion of the hydrolysis curve.

Rates of hydrolysis of the inactivated acyl-enzyme species (k_{rec}), and the attendant recovery of activity, were measured under conditions of excess substrate (0.5 mM cephaloridine) (11). A solution of a given inactivator in *p*-dioxane (typically 300 μM final concentration) was mixed with the NMC-A β-lactamase (0.7 μM final concentration). The mixture was incubated (30 min to 6 h, depending on the inhibitor) at room temperature until residual enzyme activity was less than 2%. A 10-μl portion of this mixture was added to the solution of cephaloridine (0.5 mM) in 100 mM sodium phosphate, pH 7.0. Hydrolysis of cephaloridine was monitored at 290 nm ($\Delta\epsilon_{290}$ = 2070 M^{-1} cm^{-1}). The computation of the rate constant was performed according to the method of Glick *et al.* (12).

Michaelis-Menten parameters for turnover (K_m and k_{cat}) for compounds **1-4** were evaluated by Lineweaver-Burk plots. The concentrations of the compounds were varied from 2.5 to 15 μM. A portion of the enzyme was added to a solution of the inhibitor to give a final concentration of 4 nM for the enzyme in a total volume of 1.0 ml; hydrolysis was monitored at 240 nm (**1,** $\Delta\epsilon_{240}$ = 11,480 M^{-1} cm^{-1}; **2,** $\Delta\epsilon_{240}$ = 6140 M^{-1} cm^{-1}; **3,** $\Delta\epsilon_{240}$ = 12,700 M^{-1} cm^{-1}; **4,** $\Delta\epsilon_{240}$ = 15,100 M^{-1} cm^{-1}).

Determination of the X-ray Structure of the Enzyme Inhibited by Compound **6**—Crystals of NMC-A (8) were soaked in 2 μl of a freshly prepared solution of the inhibitor containing 10 mM of **6** in 19% polyethylene glycol 1500, 190 mM MES, pH 5.25, and 10% (v/v) *p*-dioxane at 4 °C. After 15 min, crystals were mounted in cryoloops and were flash-frozen in a stream of nitrogen gas cooled to 120 K. A 1.95-Å data set was collected on the W32 wiggler beam line at LURE-DCI (Orsay, France), tuned at a wavelength of 0.97 Å, and equipped with a large MarResearch imaging plate. The crystal to detector distance was set to 270 mm. A total of 60 frames (1.5° oscillation per frame and 10-min exposure) were collected from a single NMC-A crystal. Data were processed with MOSFLM (13) and CCP4 (14) packages (Table I). The space group was $P2_12_12$ with cell parameters a = 77.48 Å, b = 52.69 Å, c = 67.10 Å. There is one molecule per asymmetric unit. The structure was refined with the program X-PLOR, version 3.1 (15), applying a bulk solvent correction. A total of 5% of the reflections were randomly selected in order to provide a test set for the R_{free} calculations (16). These reflections were omitted during refinement, but were included in the electron density map calculations. Models and electron density maps were displayed with the program TURBO FRODO (17).

Molecular replacement calculations, carried out with the AMoRe program (18) using the 1.64-Å refined NMC-A β-lactamase structure (8) as a model, were performed to account for the 1.2-Å variation of the cell parameters along the crystallographic a axis. Rigid body refinement, performed between 8.0 and 3.0 Å (R_{factor} = 0.36), was followed by molecular dynamics refinement in the resolution range 31.2–1.95 Å, using a slow cooling protocol starting from 3000 K, energy minimization, and individual thermal factor refinement. Water molecules were added as neutral oxygen atoms when they appeared as positive peaks above 4.0 σ in the $(F_{obs} - F_{calc})\exp(i\alpha_{calc})$ map in acceptable hydrogen-bonding geometry. Hereafter, the simulated annealing was performed from 500 K. The electron density maps revealed two conformations for the inhibitor covalently bound in the active site to Ser-70. The starting geometry of the inhibitor was obtained by optimization using DISCOVER (MSI). The final model of the enzyme−inhibitor complex, composed of all protein atoms with the exception of the solvent-exposed side chains of three lysine residues, includes 266 crystallographic water molecules and three molecules of MES buffer molecules. Alternate conformations were assigned to two side chains. The average B factors were 11.7 $Å^2$ for protein atoms (10.5 $Å^2$ and 12.9 $Å^2$ for main chains and side chains, respectively), 17.2 $Å^2$ for Ser-70 acylated by **6,** 23.1 $Å^2$ for solvent atoms, and 58.8 $Å^2$ for MES buffer atoms. The final crystallographic R and R_{free} values were 0.179 and 0.226, respectively.

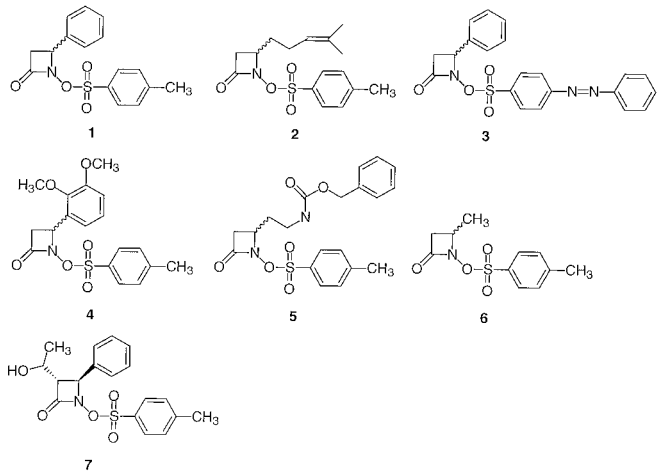

SCHEME 1. **Chemical structuring of compounds 1–7.**

Molecular Modeling and Dynamics Simulations—The coordinates of the native NMC-A β-lactamase were obtained by removing the bound inhibitor from the active site of the enzyme in the x-ray structure. This native structure was utilized to construct an immediate acyl-enzyme species for structure **11.** The immediate acyl-enzyme species refers to what would be generated after serine acylation, whereby the ester carbonyl is ensconced in the oxyanion hole with strong hydrogen bonds to the backbone amines of Ser-70 and Ser-237. There is ample structural evidence for the existence of such a species from our earlier work (19, 20). The model for the immediate acyl-enzyme intermediate included the crystallographic waters and an additional box of water molecules up to 8-Å thickness from the surface of the enzyme. The model was energy-minimized and was utilized for the molecular dynamics simulations as the starting conformation. Molecular dynamics were performed using the Amber 5.0 software package (Oxford Molecular Inc.) (21, 22), at constant pressure using periodic boundary conditions. Calculations were performed on a Silicon Graphics Octane workstation, and the graphical analysis was performed using the SYBYL molecular modeling software version 6.4 (23). The complete system was warmed from 0 to 300 K in steps of 20 K per 5 ps and then equilibrated at 300 K for 25 ps (a total of 100 ps). Snapshots of the structures were collected from here on for every 0.2 ps for 128 ps, and the resulting structures were analyzed.

RESULTS AND DISCUSSION

Kinetics—Compounds **1–7** (see Scheme 1) were tested for inhibition of the NMC-A β-lactamase. It was demonstrated (Table II) that some of the compounds of this group indeed inhibited the NMC-A β-lactamase, such as we had reported for the TEM-1 β-lactamase previously (10). Although the behavior of the two enzymes in inhibition by the monobactams shared some features, there were significant differences. Surprisingly, compound **1**, which is an excellent inhibitor of the TEM-1 β-lactamase, failed to demonstrate any inhibition of the NMC-A enzyme, but appears to be a good substrate (k_{cat}/K_m =

TABLE II
Kinetic parameters for the NMC-A β-lactamase with monobactam compounds

Compounds	$k_{inact}/[I]$	k_{rec}	k_{cat}	K_m
	$M^{-1}\ s^{-1}$	s^{-1}	s^{-1}	μM
1	[a]	[a]	120 ± 40	21 ± 7
2	710 ± 50	>0.1[b]	46 ± 18	25 ± 10
3	110 ± 30	>0.1[b]	6 ± 1	15 ± 4
4	(1.6 ± 0.4) 10^3	(9 ± 1) 10^{-3}	65 ± 25	9 ± 4
5	8 ± 2	(1.2 ± 0.2) 10^{-3}	[c]	[c]
6	130 ± 20	[d]	[c]	[c]
7	3.4 ± 0.8[e] (9 ± 1) 10^{-2} [e]	(3.2 ± 0.3) 10^{-3}	[c]	[c]

[a] No time-dependent loss of enzyme activity was detected.
[b] These values are estimates.
[c] Determination of turnover parameters was impossible.
[d] No recovery of enzyme activity was detected.
[e] Process of inactivation showed biphasic character.

(5.7 ± 0.4) $\times$ 10^6 M^{-1} s^{-1}). Compound **6** inhibits the TEM-1 β-lactamase poorly (10). In contrast, compound **6** gave rapid and irreversible loss of activity in the case of the NMC-A enzyme. We could not detect any recovery of activity from inhibition by this compound for which a rate constant could be measured (Table II). Hence, the inhibited enzyme was used in analysis of structure by x-ray diffraction (see below). Compound **3** is among the best inhibitors of the TEM-1 β-lactamase in terms of the rapidity of the inactivation process, as well as the stability of inhibited species. The NMC-A enzyme hydrolyzes this compound quite efficiently, although some transient inhibition was observed. Finally, compound **7** demonstrated a biphasic pattern of inactivation, similarly to the case of the TEM-1 enzyme (24).

X-ray Structure Determination and Refinement—The structure of the enzyme in the inhibited complex is identical to that of the native protein (8). A global superimposition of both structures based on all atoms led to a rms deviation of 0.17 Å.

Based on the first mechanistic report on this type of enzyme inactivator (10), it is expected that Ser-70 acylation by inhibitor **6** would give rise to species **8,** which would eliminate the tosyl group to arrive at species **9** (see Scheme 2). The iminium species **9** may tautomerize to enamine **10**. In turn, **9** may undergo hydrolysis of its iminium group to give the keto derivative **11,** which also may exist in its tautomeric form **12**.

The x-ray structure revealed that the catalytic Ser-70 is acylated by the inhibitor, and two different binding modes of the same molecular species were observed. The electron density indicated that the atoms of the bound inhibitor were not in the same plane, an observation that excludes structures **10** and **12**. The structural information is consistent with either the iminium species **9** or the keto species **11** as the entity resulting in enzyme inhibition. However, we are inclined to favor the keto derivative **11** as the enzyme-bound species. We conclude so because the imine moiety in **9** is fully exposed to the aqueous medium as seen in the x-ray crystal structure, and it is likely to undergo hydrolysis readily in the absence of any specific interactions with the enzyme active site that would stabilize the iminium group. The identical position for the hydroxyl group of Ser-130 in the structures of the native enzyme and in the inhibited complex is suggestive of a noncharged group, such as the ketone moiety of **11** in its vicinity.

As indicated earlier, the electron density is consistent with two bound conformations for the inhibitor in the active site (Fig. 1). In conformation I (Fig. 1, *A* and *C*), the oxygen atom of the ester is located at 2.6 Å and 3.2 Å from the main chain nitrogen atoms of residues 70 and 237, respectively. The oxygen atom of the ketone group of **11** forms a hydrogen bond to the side chain of Ser-130 (2.7 Å). In conformation II of the

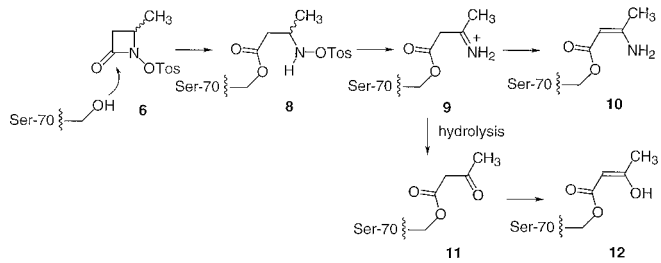

SCHEME 2. **Mechanism of inhibition of β-lactamase by inhibitor.**

bound inhibitor, the carbonyl oxygen atom of the ester is at hydrogen-bonding distance to the hydroxyl group of Ser-130 (3.0 Å), and the oxygen of the ketone is hydrogen-bonded to the Nδ2 atom of Asn-132 (Fig. 1, *B* and *C*). The water molecule implicated in the deacylation reaction is found in a similar position as in the native enzyme structure. It has a full occupancy according to the refinement criteria. However, the water molecule does not seem to be in a good position to attack the ester moiety, in either conformation observed in the x-ray crystal structure. Conformation I of the complex is not positioned ideally within the oxyanion hole, such as documented previously for other acyl-enzyme intermediates (9, 20). So, despite the ester carbonyl being still sequestered in the oxyanion hole, the hydrolytic water is held almost within the plane formed by the ester moiety in the active site. In other words, the angle of attack for the activated water (160° in conformation I, at a distance of 3.2 Å) is not favorable (Fig. 1*A*). In conformation II, the ester carbonyl moiety is not held in the oxyanion hole, and also the angle for attack of the hydrolytic water is 148° at a distance of 3.3 Å (Fig. 1*B*). Thus, in neither conformation does the acylated enzyme species appear to be in a position to undergo hydrolysis by the promoted hydrolytic water. Furthermore, the occupancy of the energy minima represented by conformations I and II of the inhibited enzyme species must be high enough so that high resolution x-ray structure of the complex could be solved and that the inhibited species does not undergo hydrolysis allowing for the recovery of activity.

Molecular Dynamics Simulations—Recently we performed molecular dynamics simulations to understand the dynamic nature of the acyl-enzyme intermediate for imipenem, a carbapenem antibiotic, bound to the active site of TEM-1 β-lactamase (19). These studies revealed that the ester carbonyl for the immediate acyl-enzyme intermediate for the TEM-1 β-lactamase moved out of the oxyanion hole in the picosecond time scale. Furthermore, the ester carbonyl was capable of returning into the oxyanion hole in a time-dependent manner. We had proposed in our report that the simulations demonstrated that the acyl-enzyme complexes of the β-lactamases are not rigid structures and would undergo dynamic motion in and out of the active site oxyanion hole. Experimental demonstration of such a motion had not been made prior to this work, as the alternative conformation needs to be relatively stable to survive and be detected by various means, in our case by x-ray structure determination. The existence of the two conformations for the inhibitor **6** bound in the active site of the NMC-A β-lactamase illustrates the motion for the ester carbonyl in and out of the oxyanion hole. It underscores the importance of the dynamic aspect of these intermediary species to the catalytic processes of β-lactamases.

Molecular dynamics simulations were performed to better understand the nature of the motions of the inhibited species in the active site of the NMC-A β-lactamase and to explain the observation of the two conformations in the x-ray structure analyses. These simulations started from the structure of the so-called immediate acyl-enzyme intermediate, which is the

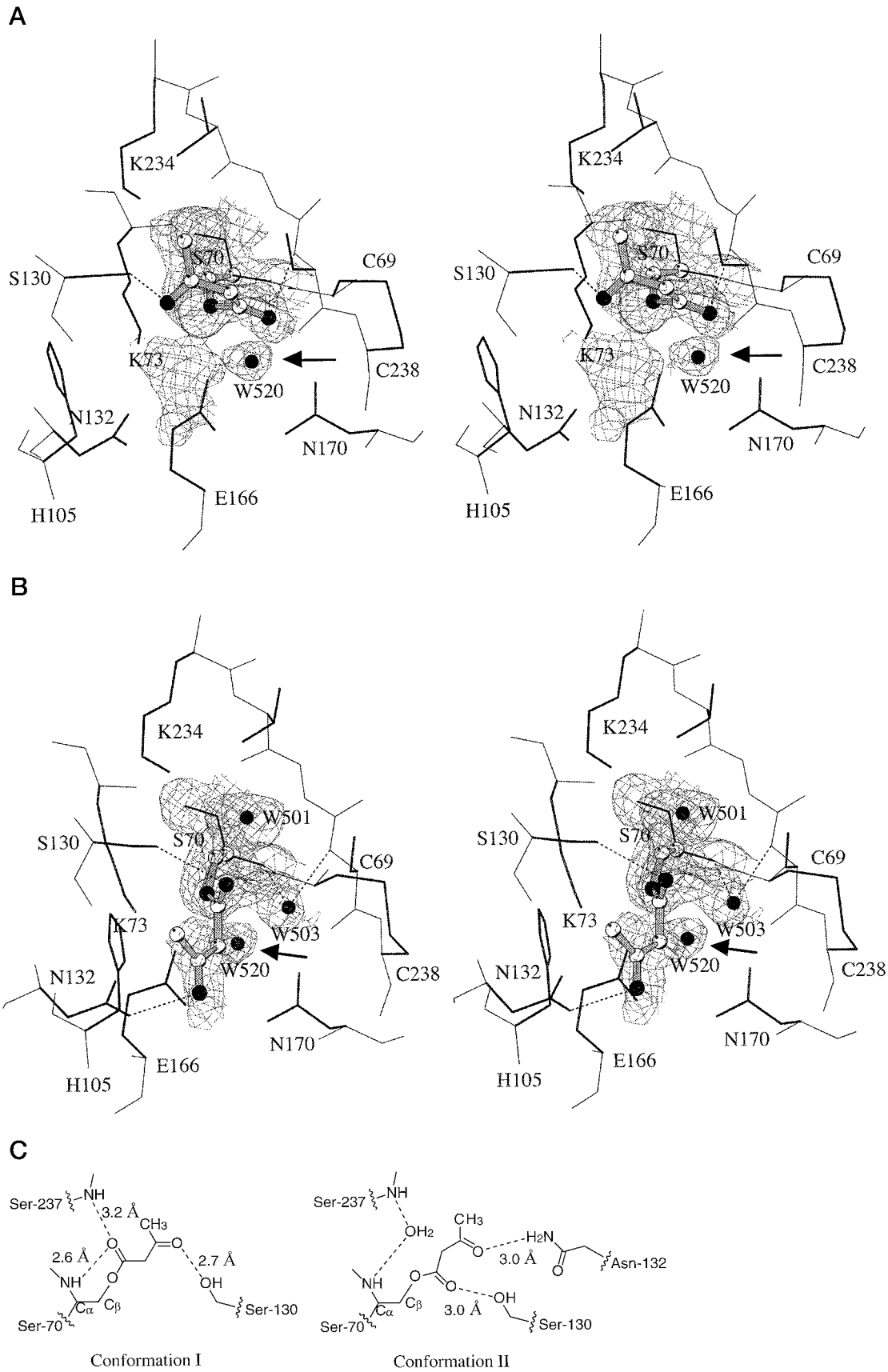

FIG. 1. **Stereo views of the x-ray structure of the NMC-A β-lactamase inhibited by the monobactam 6.** Electron density maps of the acyl-enzyme intermediate (species **11**) in conformation I (*A*) and in conformation II (*B*). In *B*, the oxyanion hole is occupied by a water molecule ("*W503*"), shown here as a *sphere*. In *A* and *B*, the inhibitor molecule is shown in the *ball-and-stick* representation, and the hydrolytic water molecule ("*W520*") is shown as a *sphere*. *C*, schematic of the two different conformations for species **11.**

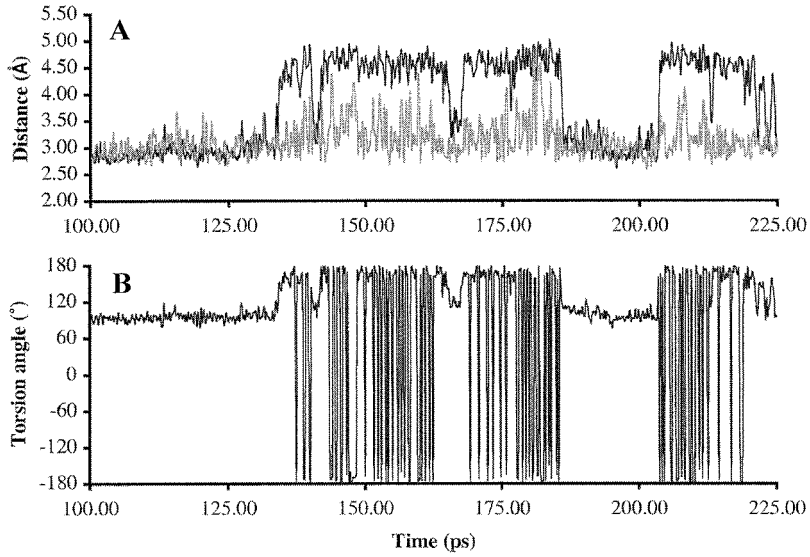

FIG. 2. *A*, the distance versus time profiles for the molecular dynamics simulations of the acyl-enzyme species of the complex of compound **6** and the NMC-A β-lactamase. The *black* and *gray lines* show the distances between the acyl carbonyl oxygen and the backbone amine of Ser-70 and that of Ser-237, respectively. *B*, the conformational space sampled by the C_α-C_β-O-C torsion angle in the enzyme-inhibitor complex is shown as a function of time.

direct product of active site serine acylation of the enzyme by the β-lactam entity.

The distances of the ester carbonyl oxygen from the backbone nitrogen of Ser-70 and that of Ser-237 are plotted as a function of time (in picoseconds) in Fig. 2*A*. During the initial 135 ps of the simulations (including the warm-up and equilibration periods), we observed that the hydrogen bond distances in the oxyanion hole are maintained around 3 Å. At 133 ps, the hydrogen bond between the carbonyl oxygen and the backbone nitrogen of Ser-70 broke (*dark line* in Fig. 2*A*). However, this hydrogen bond formed again at 187 ps. The other hydrogen bond, that between the carbonyl group of the ester moiety and the backbone nitrogen of Ser-237 (*gray line* in Fig. 2A) broke and reformed several times from 136–187 ps of the simulation period. At approximately 187 ps, both hydrogen bonds were reformed, and the conformation of the complex at this point was similar to that of the immediate acyl-enzyme species (the initial starting conformation for simulations). However, at approximately 203 ps of simulations (*i.e.* 16 ps subsequent to its re-entry into the oxyanion hole) the ester moiety showed motion out of the oxyanion hole. Both hydrogen bonds with the oxyanion hole broke and reformed several times from this point on to the end of the simulations.

We analyzed the structures of the snapshots that were collected during the simulations, and the conformational space sampled by the C_α-C_β-O-C torsion angle in the enzyme-inhibitor complex was plotted as a function of time (Fig. 2*B*; the "C_α-C_β-O" portion belongs to Ser-70 and the carbon attached to oxygen is that of the inhibitor; see Fig. 1*C*). This torsion angle determines the orientation of the ester moiety in the active site of the enzyme. During the simulations, the above torsion angle assumes values close to 140° (for example, at 140 ps in Fig. 2*B*), where both the oxyanion hole hydrogen bonds are lost. This geometry is close to conformation II that was observed experimentally in the x-ray structure (C_α-C_β-O-C torsion angle 142° in Fig. 1*C*). The other experimentally observed conformation (conformation I) possesses a C_α-C_β-O-C torsion angle of 73°, different than that for the immediate acyl-enzyme species (93°; the starting point for simulations), which should be prone to deacylation. Interestingly, we found that the torsion angle corresponding to that for conformation I is sampled for a reasonable duration of the simulation (Fig. 2*B*). We observe in Fig. 2*B* that the ester moiety assumes various positions in the active site, including the ones in the oxyanion hole. The two conformations that were observed in the x-ray analysis can be rationalized as two highly populated conformations of the acyl-enzyme species. Any conceivable hydrolysis of these species depends on the stability of the conformation(s) with ester oxygen in the oxyanion hole, as well as the proper orientation for attack by the activated hydrolytic water (see above). Consistent with the x-ray structure and the dynamics simulations, which refute the possibility for deacylation of the inhibited species, we did not see any detectable deacylation in kinetics experiments either.

We have demonstrated in this manuscript that structurally simple monobactam molecules can serve as very effective inhibitors for the broad spectrum NMC-A β-lactamase, and the x-ray structure of the inhibited enzyme has shed light on the mechanism of inhibition. It is interesting to note that the mere presence of a small portion of the inhibitor in covalent liaison with the active site serine allows the existence of two low-energy species, which do not undergo deacylation with the attendant recovery of enzyme activity. Molecular dynamics simulations have underscored the existence of considerable structural flexibility for the inhibited enzyme species, a process that allowed for the observations of the two species seen in the x-ray structure of the inhibited enzyme as important entities in the course of simulations. This structural dynamic nature is probably present in other acyl-enzyme intermediates for β-lactamases such as recently documented for another β-lactamase (25). Since simulations indicate the possibility of such motion in picosecond time scale and the fact that catalysis by these enzymes take place on millisecond time scale, it is likely that such dynamic motion takes place with typical substrates for these enzymes as well. However, structural properties of substrates would prevent their acyl-enzyme species from being trapped in energy minima that would result in enzyme inhibition, such as demonstrated here in our report.

Acknowledgments—The use of the Lizzadro Magnetic Resonance Center for the NMR studies at the University of Notre Dame is gratefully acknowledged. We thank Valérie Guillet for her excellent assistance in data collection. The beam line staff at LURE is gratefully acknowledged for the facility placed at our disposal.

REFERENCES

1. Bush, K., and Mobashery, S. (1998) in *Resolving the Antibiotic Paradox: Progress in Understanding Drug Resistance and Development of New Antibiotics* (Rosen, B. P., and Mobashery, S., eds) pp. 71–98, Plenum Press, New York
2. Matagne, A., Lamotte-Brasseur, J., and Frère, J.-M. (1998) *Biochem. J.* **330,** 581–598
3. Hardy, L. W., and Kirsch, J. F. (1989) *Arch. Biochem. Biophys.* **268,** 338–348
4. Nordmann, P., Mariotte, S., Naas, T., Labia, R., and Nicolas, M. H. (1993) *Antimicrob. Agents Chemother.* **37,** 939–946
5. Naas, T., Vandel, L., Sougakoff, W., Livermore, D. M., and Nordmann, P.

(1994) *Antimicrob. Agents Chemother.* **38,** 1262–1270
6. Rasmussen, B. A., Bush, K., Keeney, D., Yang, Y., Hare, R., O'Gara, C., and Medeiros, A. A. (1996) *Antimicrob. Agents Chemother.* **40,** 2080–2086
7. Rasmussen, B. A., and Bush, K. (1997) *Antimicrob. Agents Chemother.* **41,** 223–232
8. Swarén, P., Maveyraud, L., Raquet, X., Cabantous, S., Duez, C., Pedelacq, J. D., Mariotte-Boyer, S., Mourey, L., Labia, R., Nicolas-Chanoine, M. H., Nordmann, P., Frère, J. M., and Samama, J. P. (1998) *J. Biol. Chem.* **273,** 26714–26721
9. Mourey, L., Miyashita, K., Swarén, P., Bulychev, A., Samama, J. P., and Mobashery, S. (1998) *J. Am. Chem. Soc.* **120,** 9382–9383
10. Bulychev, A., O'Brien, M. E., Massova, I., Teng, M., Gibson, T. A., Miller, M. J., and Mobashery. S. (1995) *J. Am. Chem. Soc.* **117,** 5938–5943
11. Koerber, S. C., and Fink, A. L. (1987) *Anal. Biochem.* **165,** 75–87
12. Glick, B. R., Brubacher, L. J., and Leggett, D. J. (1978) *Can. J. Biochem.* **56,** 1055–1057
13. Leslie, A. G. W. (1992) *Joint Collaborative Computing Project 4 and European Science Foundation-European Association of the Crystallography of Biological Macromolecules Newsletter on Protein Crystallography*, Vol. 26, SERC Daresbury Laboratory, Warrington, UK
14. Collaborative Computational Project Number 4 (1994) *Acta Crystallogr. Sect. D* **50,** 760–763
15. Brünger, A. T. (1992) *X-PLOR, A System for X-ray Crystallography and NMR*, version 3.1, Yale University Press, New Haven, CT
16. Brünger, A. T. (1992) *Nature* **355,** 472–475
17. Roussel, A., Inisan, A.-G., and Cambillau, C., TURBO FRODO program, AFMB and Biographics, Marseille, France
18. Navaza, J. (1994) *Acta Crystallogr. Sect. A* **50**, 157–163
19. Maveyraud, L., Mourey, L., Kotra, L. P., Pédelacq, J. D., Guillet, V., Mobashery, S., and Samama, J. P. (1998) *J. Am. Chem. Soc.* **120,** 9748–9752
20. Maveyraud, L., Massova, I., Birck, C., Miyashita, K., Samama, J.-P., and Mobashery, S. (1996) *J. Am. Chem. Soc.* **118,** 7435–7440
21. Case, D. A., Pearlman, D. A., Caldwell, J. W., Cheatham, T. E., III, Ross, W. S., Simmerling, C. L., Darden, T. A., Merz, K. M., Stanton, R. V., Cheng, A. L., Vincent, J. J., Crowley, M., Ferguson, D. M., Radmer, R. J., Seibel, G. L., Singh, U. C., Weiner, P. K., and Kollman, P. A. (1997) *AMBER 5*, University of California, San Francisco, CA
22. Pearlman, D. A., Case, D. A., Caldwell, J. W., Ross, W. S., Cheatham, T. E., III, DeBolt, S., Ferguson, D., Seibel, G., and Kollman, P. A. (1995) *Comp. Phys. Commun.* **91,** 1–41
23. *SYBYL, Molecular Modeling Software*, version 6.4, Tripos Associates, St. Louis, MO
24. Swarén, P., Massova, I., Bellettini, J.m Bulychev, A., Maveyraud, L., Kotra, L. P., Miller, M. J., Mobashery, S., and Samama, J. P. (1999) *J. Am. Chem. Soc.* **121,** 5353–5359
25. Wilkinson, A. S., Ward, S., Kania, M., Page, M. G. P., and Wharton, C. W. (1999) *Biochemistry* **38,** 3851–3856

Inhibition of the Broad Spectrum Nonmetallocarbapenamase of Class A (NMC-A) β -Lactamase from *Enterobacter cloacae* by Monocyclic β-Lactams

Lionel Mourey, Lakshmi P. Kotra, John Bellettini, Alexey Bulychev, Michael O'Brien, Marvin J. Miller, Shahriar Mobashery and Jean-Pierre Samama

J. Biol. Chem. 1999, 274:25260-25265.
doi: 10.1074/jbc.274.36.25260